Articles

Rates of the Oxidative Addition of Benzyl Halides to a Metallacyclic Palladium(II) Complex and of the Reductive Elimination from a Benzyl-Palladium(IV) Complex

Christian Amatore,*[,†] Marta Catellani,*[,‡] Sara Deledda,[†] Anny Jutand,*[,†] and Elena Motti[‡]

Département de Chimie, Ecole Normale Supérieure, UMR ENS-CNRS-UPMC 8640, 24 Rue Lhomond, F-75231 Paris Cedex 5, France, and Dipartimento di Chimica Organica e Industriale dell'Università degli Studi di Parma, Viale G.P. Usberti, 17/A, I-43100, Parma, Italy

Received January 7, 2008

Pd(II) metallacyclic complexes are key intermediates in sequential reactions in which three new C−C bonds are formed in an aromatic ring. The Pd(II) metallacyclic complex **10** with phenanthroline as ligand undergoes oxidative addition to benzyl bromide or chloride in DMF to generate benzyl-Pd(IV) complexes. The rate constant of the oxidative addition is determined by means of electrochemical techniques, with the expected reactivity order $PhCH_2Br$ ($k_{1Br} = 3.6\ M^{-1}\ s^{-1}$) > $PhCH_2Cl$ ($k_{1Cl} = 6 \times 10^{-3}\ M^{-1}\ s^{-1}$) at 29 °C. When the benzyl-Pd(IV) complex is generated from $PhCH_2Br$, the oxidative addition is followed by a slow C−C reductive elimination, which gives a Pd(II) complex. The rate constant of the reductive elimination has been determined in DMF ($k_{2Br} = 6 \times 10^{-4}\ s^{-1}$) at 29 °C.

Introduction

Selective aromatic functionalization by means of transition metal complexes is an important topic to which palladium chemistry has contributed significantly. In particular, palladacycles have been proved to be quite valuable to this goal in providing a facile way for the activation of an aromatic ring.[1] Some of us have intensively investigated this area and reported a new methodology for selective aromatic alkylation and arylation based on the catalytic activity of palladium and norbornene.[2]

Scheme 1 reports an example of a sequential one-pot reaction in which three new C−C bonds are formed with selective functionalization of two mutually *meta* positions of an aromatic ring. As a result, an *ortho*,*ortho*′-disubstituted vinylarene is formed.[3]

Scheme 1

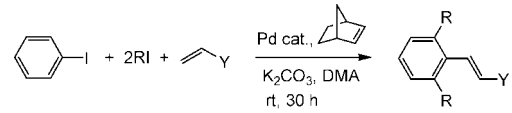

Scheme 2

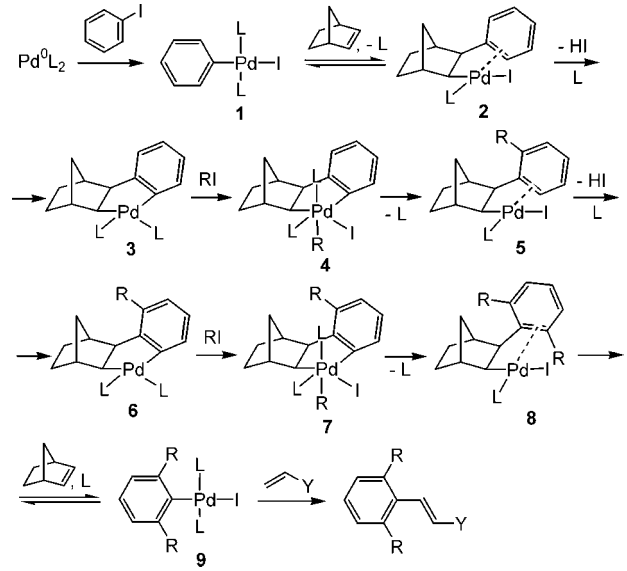

Scheme 2 reports the proposed reaction pathway that shows the important role played by palladium(II) and palladium(IV) metallacycles **3**, **4**, **6**, and **7**.[3] The *cis,exo* arylnorbornylpalladium(II) species **2** is formed by oxidative addition of iodobenzene to palladium(0) and subsequent stereoselective norbornene insertion into the resulting arylpalladium complex **1**.[4] Ring

* To whom correspondence should be addressed. Fax: (+33) 1-44-32-24-02. E-mail: Anny.Jutand@ens.fr; christian.amatore@ens.fr; marta.catellani@unipr.it.

† Ecole Normale Supérieure.

‡ Università degli Studi di Parma.

(1) (a) Tamao, K. In *Comprehensive Organic Synthesis*; Trost, B. M., Fleming, I., Eds.; Pergamon: Oxford, 1991; Vol. 3, pp 435−480. (b) Leong, W. W.; Larock, R. C. In *Comprehensive Organometallic Chemistry, II*; Abel, E. W., Stone, G., Wilkinson, G., Eds.; Pergamon: Oxford, 1995; Vol. 12, pp 131−160. (c) Dyker, G. *Angew. Chem., Int. Ed.* **1999**, *38*, 1698–1712. (d) Luh, T.-Y.; Leung, M.-K.; Wong, K.-T. *Chem. Rev.* **2000**, *100*, 3187–3204. (e) Ryabov, A. D. *Chem. Rev.* **1990**, *90*, 403–424. (f) Beletskaya, I. P.; Cheprakov, A. V. *J. Organomet. Chem.* **2004**, *689*, 4055–4082. (g) Dupont, J.; Consorti, C. S.; Spencer, J. *Chem. Rev.* **2005**, *105*, 2527–2572.

(2) (a) Catellani, M. *Synlett* **2003**, 298–313. (b) Catellani, M. *Top. Organomet. Chem.* **2005**, *14*, 21–53. (c) Catellani, M.; Motti, E.; Faccini, F.; Ferraccioli, R. *Pure Appl. Chem.* **2005**, *77*, 1243–1248. (d) Catellani, M.; Motti, E. In *Handbook of C−H Transformations*; Dyker, G., Ed.; Wiley-VCH: Weinhein, 2005; Vol. 1, pp 245−251. (e) Faccini, F.; Motti, E.; Catellani, M. *J. Am. Chem. Soc.* **2004**, *126*, 78–79.

10.1021/om800015x CCC: $40.75
Publication on Web 08/20/2008

closure through aromatic C−H activation[5] leads to palladacycle **3**.[6] Oxidative addition of alkyl iodide to **3** gives the metallacycle complex of palladium(IV), **4**, which undergoes a reductive elimination by selective migration of the R group to the aromatic site of the palladacycle.[3,7] The resulting arylnorbornylpalladium species **5** behaves analogously to the precursor **2**, undergoing (a) ring closure to **6**; (b) oxidative addition of a new molecule of alkyl iodide to form the palladium(IV) species **7**; and (c) reductive elimination to give **8**. Likely due to the steric effect of norbornene, expulsion occurs at this stage, leading to the *o,o′*-disubstituted arylpalladium complex **9**, which undergoes Heck reaction to give the final organic product. Among the many interesting aspects of this catalytic cycle, the role played by alkylaromatic metallacycles of palladium(II) and (IV) is worth noting. The formation of palladacycles **3** and **6** allows C−H bond activation, while through metallacycles of palladium(IV), **4** and **7**, selective alkylation becomes possible. The reaction scope has been largely explored using a variety of aromatic compounds, organic halides, and terminating agents. Among the latter arylboronic acids, hydrogen transfer agents and acetylenic compounds have been used besides olefins.[2,8]

Lautens et al. also reported interesting extensions of this sequential reaction. Using an alkyl halide containing an olefinic group, they could obtain cyclic compounds through an intramolecular Heck reaction and several other accomplishments concerning sequential reactions involving C−C bond formation and C−H activation.[9]

In view of the potential of these metallacycle-driven reactions, we have deemed useful to study the reactivity of the model palladacycle **10**, containing phenanthroline as ligand, in reactions with benzyl halides, which readily give oxidative addition.[7] The kinetics of the C−C reductive elimination that follows the oxidative addition has been investigated as well.

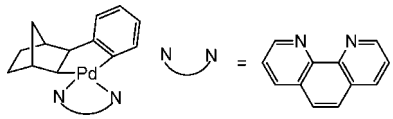

10

Results and Discussion

Kinetics of the Oxidative Addition of Benzyl Halides to the Pd(II) Complex 10. The Pd(II) complex **10** (3 mM) was characterized by cyclic voltammetry in DMF containing nBu$_4$NBF$_4$ (0.3 M). It exhibited three reduction peaks (Figure 1a). The first reversible one, R_1, at $E^p_{R1} = -1.505$ V vs SCE, characterizes the monoelectronic reduction of the phenanthroline ligated to the Pd(II) center. The second one, R_2, at $E^p_{R2} = -2.255$ V vs SCE, was irreversible. It reduction peak current was about twice that of R_1, indicating an overall two-electron reduction. It is followed by a third tiny reversible reduction peak at $E^p_{R3} = -2.430$ V vs SCE.[10]

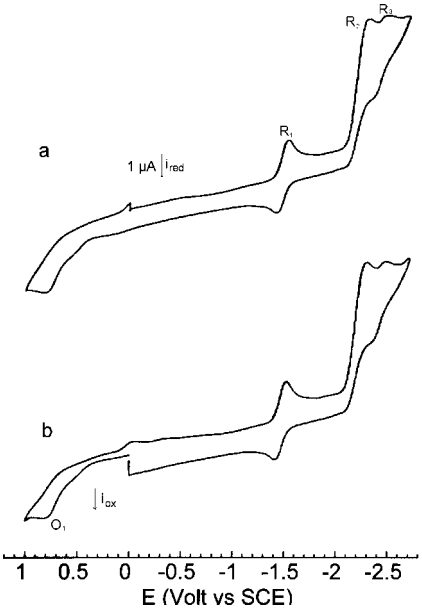

Figure 1. Cyclic voltammetry of complex **10** (3 mM) in DMF (containing nBu$_4$NBF$_4$, 0.3 M) at a steady gold disk electrode (d = 0.5 mm) and a scan rate of 0.5 V s^{-1} at 25 °C. (a) Reduction first. (b) Oxidation first.

More interestingly, the Pd(II) complex **10** exhibited an irreversible oxidation peak O_1 at $E^p_{O1} = +0.795$ V vs SCE preceded by a prewave (Figure 1b).[11]

When an excess of $PhCH_2Br$ was added to the Pd(II) complex **10**, the oxidation peak O_1 disappeared with time, suggesting that a reaction proceeded between the two reagents, presumably

(3) (a) Catellani, M.; Frignani, F.; Rangoni, A. *Angew. Chem., Int. Ed. Engl.* **1997**, *36*, 119–122, and references therein. (b) Catellani, M.; Fagnola, M. C. *Angew. Chem., Int. Ed. Engl.* **1994**, *33*, 2421–2422.

(4) (a) Horino, H.; Arai, M.; Inoue, N. *Tetrahedron Lett.* **1974**, 647–650. (b) Portnoy, M.; Ben-David, Y.; Rousso, I.; Milstein, D. *Organometallics* **1994**, *13*, 3465–3479. (c) Li, C.-S.; Cheng, C.-H.; Liao, F.-L.; Wang, S.-L. *Chem. Commun.* **1991**, 710–712. (d) Catellani, M.; Mealli, C.; Motti, E.; Paoli, P.; Perez-Carreno, E.; Pregosin, P. S. *J. Am. Chem. Soc.* **2002**, *124*, 4336–4346.

(5) (a) Dyker, G. *Handbook of CH Transformation*; Wiley-VCH: Weinheim, 2005. (b) Dyker, G. *Angew. Chem., Int. Ed.* **1999**, *38*, 1698–1712.

(6) (a) Catellani, M.; Chiusoli, G. P. *J. Organomet. Chem.* **1988**, *346*, C27−C30. (b) Catellani, M.; Marmiroli, B.; Fagnola, M. C.; Acquotti, D. *J. Organomet. Chem.* **1996**, *507*, 157–162. (c) Dyker, G. *Chem. Ber.* **1997**, *130*, 1567–1578. (d) Cámpora, J.; Palma, P.; Carmona, E. *Coord. Chem. Rev.* **1999**, *193−195*, 207–281.

(7) (a) Catellani, M.; Mann, B. E. *J. Organomet. Chem.* **1990**, *390*, 251–255. (b) Bocelli, G.; Catellani, M.; Ghelli, S. *J. Organomet. Chem.* **1993**, *458*, C12−C15.

(8) (a) Catellani, M.; Cugini, F. *Tetrahedron* **1999**, *55*, 6595–6602. (b) Catellani, M.; Motti, E.; Minari, M. *Chem. Commun.* **2000**, 157–158. (c) Catellani, M. *Pure Appl. Chem.* **2002**, *74*, 63–68.

(9) (a) Lautens, M.; Piguel, S. *Angew. Chem., Int. Ed.* **2000**, *39*, 1045–1046. (b) Alberico, D.; Scott, M. E.; Lautens, M. *Chem. Rev.* **2007**, *107*, 174–238. (c) Mariampillai, B.; Alliot, J.; Li, M.; Lautens, M. *J. Am. Chem. Soc.* **2007**, *129*, 15372–15379.

(10) Our purpose was not to investigate the mechanism of the reduction of complex **10** and to determine the structure of the complexes formed after the successive electron transfers. However, one may assume that the first reversible reduction process at R_1 involves the reduction of the phenanthroline ligand and the resulting complex **10**$^{\bullet-}$. After an overall dielectronic process at R_2, a cleavage of the two Pd−C bonds would occur with formation of the dianionic phenylnorbornyl organic ligand together with the unstable 15-electron Pd^0(phenanthroline)$^{\bullet-}$. The latter was reduced in the third reduction step at R_3 into the 16-electron complex Pd^0(phenanthroline)$^{2-}$,the two electrons being located on the phenanthroline ligand. Under similar experimental conditions, the free phenanthroline exhibited two successive reversible reduction peaks at−1.975 and−2.15 V vs SCE.

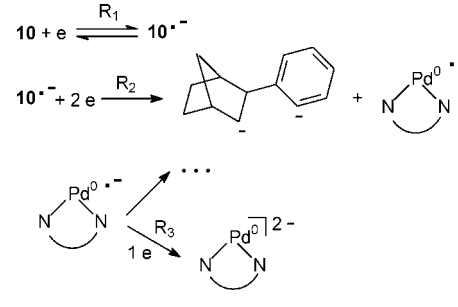

Scheme 3

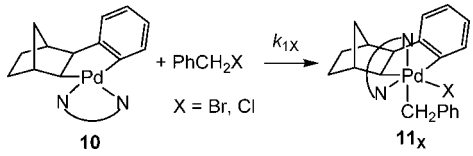

an oxidative addition that gave the Pd(IV) complex $\mathbf{11_{Br}}$ (Scheme 3). Complexes of this type have been isolated and characterized by NMR spectroscopy. Their structure in solution is fully consistent with the ligand arrangement shown in formula $\mathbf{11_X}$.[7]

The oxidative addition of $PhCH_2Br$ to the Pd(II) complex $PhCH_2PdBr(PPh_3)_2$ generates a Pd(IV) complex, $(PhCH_2)_2Pd(Br)_2(PPh_3)_2$, as proposed by Stille et al.[12] Oxidative additions of alkyl halides to Pd(II) complexes ligated to diamine or bipyridine ligands that generate Pd(IV) complexes are also reported.[13]

Kinetics of the Oxidative Addition of $PhCH_2Br$ to the Pd(II) Complex 10. The kinetics of the oxidative addition of $PhCH_2Br$ to complex **10** (C_0 = 3 mM) (rate constant k_{1Br} in Scheme 3) was monitored by amperometry performed at a rotating gold disk electrode (d = 2 mm) polarized at +1.0 V, on the oxidation wave O_1 of **10**. The decay of the oxidation current of **10** (proportional to its concentration)[14] was recorded versus time in the presence of excess $PhCH_2Br$ until total conversion. The plot of ln x against time was linear ($x = [\mathbf{10}]/[\mathbf{10}]_0 = i/i_0$ with i = oxidation current at wave O_1 at t, i_0 = initial oxidation current), attesting to a first-order reaction for complex **10** (Figure 2a).

The value of the observed rate constant k_{1Br}^{obs} of the oxidative addition was calculated from the slope of the straight line: $\ln x = -k_{1Br}^{obs}t$. It varied linearly with $PhCH_2Br$ concentration with a zero intercept (Figure 2b): $k_{1Br}^{obs} = k_{1Br}[PhCH_2Br]$, attesting to a first-order reaction for $PhCH_2Br$. The rate constant k_{1Br} was determined from the slope of the straight line of Figure 2b.

$$k_{1Br} = 3.6\ M^{-1}\ s^{-1}\ (DMF, 29\ °C) \qquad (1)$$

Kinetics of the Oxidative Addition of $PhCH_2Cl$ to the Pd(II) Complex 10. The kinetics of the oxidative addition of $PhCH_2Cl$ to the Pd(II) complex **10** was investigated under the same experimental conditions as for $PhCH_2Br$ (rate constant k_{1Cl} in Scheme 3). The oxidation current of **10** dropped to zero upon addition of excess $PhCH_2Cl$ (in the range 0.07−0.3 M). The oxidative addition of $PhCH_2Cl$ was considerably slower than that of $PhCH_2Br$ at identical concentrations. When the $PhCH_2Cl$ concentration was varied, the plot of ln x against time afforded a series of straight lines whose slopes (k_{1Cl}^{obs}) varied linearly with $PhCH_2Cl$ concentration, attesting to a first-order reaction for $PhCH_2Cl$ (Figure 3).

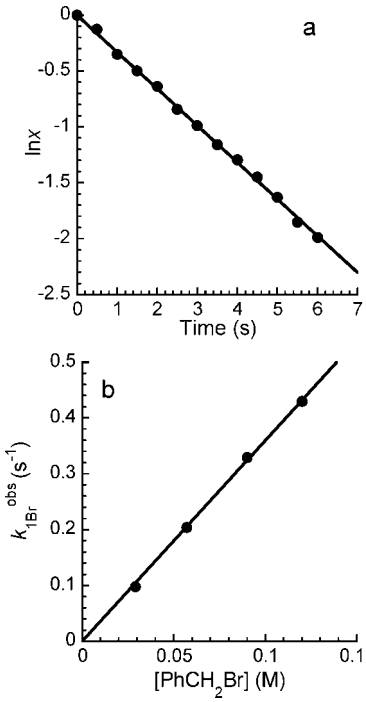

Figure 2. Kinetics of the oxidative addition of $PhCH_2Br$ to the Pd(II) complex **10** (3 mM) in DMF (containing nBu$_4$NBF$_4$, 0.3 M) at 29 °C, as monitored by amperometry at a rotating gold disk electrode (d = 2 mm) polarized at +1 V, on the oxidation wave of **10**. (a) Variations of ln x versus time ($x = [\mathbf{10}]/[\mathbf{10}]_0 = i/i_0$ with i = oxidation current at wave O_1 at t, i_0 = initial oxidation current). $[PhCH_2Br]$ = 90 mM. $\ln x = -k_{1Br}^{obs}t$. (b) Determination of the reaction order for $PhCH_2Br$: plot of k_{1Br}^{obs} versus $PhCH_2Br$ concentration. $k_{1Br}^{obs} = k_{1Br}[PhCH_2Br]$.

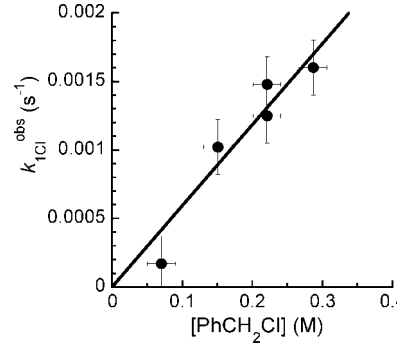

Figure 3. Kinetics of the oxidative addition of $PhCH_2Cl$ to complex **10** (3 mM) in DMF (containing nBu$_4$NBF$_4$, 0.3 M) at 29 °C. Determination of the reaction order for $PhCH_2Cl$: plot of k_{1Cl}^{obs} versus $PhCH_2Cl$ concentration. $k_{1Cl}^{obs} = k_{1Cl}[PhCH_2Cl]$.

The rate constant of the oxidative addition was determined from the slope of the straight line of Figure 3.

$$k_{1Cl} = 6\times10^{-3}\ M^{-1}\ s^{-1}\ (DMF, 29\ °C) \qquad (2)$$

$PhCH_2Br$ is then 600 times more reactive than $PhCH_2Cl$ in the oxidative addition to the Pd(II) complex **10**. The reactivity order $PhCH_2Br$ > $PhCH_2Cl$ is usual in oxidative additions to Pd(0) complexes.[12] It was also expected for oxidative additions to Pd(II) complexes. This oxidative addition gives Pd(IV) complexes $\mathbf{11_X}$ (X = Br, Cl), which, according to the mechanism proposed in Scheme 2, should undergo a C−C reductive elimination, giving back a Pd(II) complex.

(11) The mechanism of the oxidation of complex **10** has not been investigated in full detail since this was not relevant to this study. Nevertheless, we can assume that the oxidation peak O_1 of **10** involved one electron by comparison of its oxidation peak current (Figure 1b) with its reduction peak current at R_1 (reversible process, Figure 1a). O_1 was preceded by a prewave. This is characteristic of a CE mechanism in which a species that was more easily oxidized than **10** but present at very low thermodynamic concentration in an equilibrium with the main species was however detected by its oxidation peak because the equilibrium was continuously shifted toward its formation by its consumption in the diffusion layer by the electron transfer during the cyclic voltammetry performed at a low scan rate (long time scale).

(12) (a) Milstein, D.; Stille, J. K. *J. Am. Chem. Soc.* **1979**, *101*, 4992–4998. (b) Gillie, A.; Stille, J. K. *J. Am. Chem. Soc.* **1980**, *102*, 4933–4941.

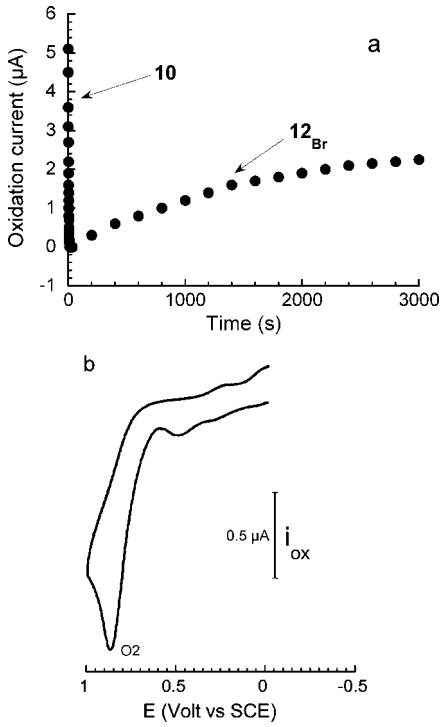

Figure 4. (a) Decrease of the oxidation current of the Pd(II) complex **10** (3 mM) in DMF (containing nBu$_4$NBF$_4$ 0.3 M) versus time, in its oxidative addition to PhCH$_2$Br (0.57 M) ($0 < t < 12$s), as monitored by amperometry at a rotating gold disk electrode ($d = 2$ mm) polarized at +1 V, at 29 °C. It is followed by the increase of the oxidation current of the Pd(II) complex $\mathbf{12_{Br}}$ generated by reductive elimination from the Pd(IV) complex $\mathbf{11_{Br}}$ formed in the previous oxidative addition. (b) Cyclic voltammetry of the Pd(II) complex $\mathbf{12_{Br}}$ generated as in Figure 4a at a steady gold disk electrode ($d = 2$ mm) at the scan rate of 0.5 V s^{-1}.

Kinetics of the C−C Reductive Elimination from the Benzyl−Pd(IV) Complex $\mathbf{11_{Br}}$. When the oxidative addition of the Pd(II) complex **10** (3 mM) was performed in the presence of a large excess of PhCH$_2$Br (0.57 M), the oxidation current of complex **10** rapidly dropped to zero, attesting to a fast oxidative addition ($0 < t < 12$ s, decreasing part of Figure 4a) with formation of the Pd(IV) complex $\mathbf{11_{Br}}$. An oxidation current was then observed that slowly increased with times ($t > 15$ s in Figure 4a). Consequently, once the fast oxidative addition was over, a new complex was formed in a slower reaction from complex $\mathbf{11_{Br}}$ and exhibited an oxidation current at +1 V vs SCE, the polarization potential of the rotating disk electrode. A cyclic voltammetry was performed once the formation of the new complex was over ($t >$ 3000 s). An oxidation peak, O_2, was indeed observed at $E^p_{O2} =$ +0.830 V vs SCE (Figure 4b), i.e., with a peak potential slightly more positive than that of the Pd(II) complex **10**. This oxidation peak is assigned to the Pd(II) complex $\mathbf{12_{Br}}$[7b] generated by a C−C reductive elimination taking place from the Pd(IV) complex $\mathbf{11_{Br}}$ (Scheme 4).[15a] Complex $\mathbf{12_{Br}}$ has been isolated in 74% yield and characterized by ^{1}H NMR as the final complex formed in a stoichiometric reaction of PhCH$_2$Br and the Pd(II) complex **10**.

Scheme 4

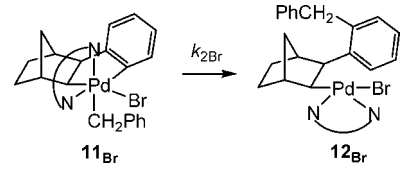

The same sequence, i.e., oxidative addition followed by C−C reductive elimination, had been observed in the reaction of **10** with *p*-nitrobenzyl bromide, leading to *p*-nitro-substituted $\mathbf{11_{Br}}$, then to *p*-nitro-substituted $\mathbf{12_{Br}}$.[7b] The C−C reductive elimination from Pd(IV) complexes ligated to diamine or bipyridine ligands has been reported by Canty et al.,[13a] van Koten et al.,[13d] and Elsevier et al.[13f]

According to Scheme 4, the increase of the oxidation current at long times observed in Figure 4a, assigned to the Pd(II) complex $\mathbf{12_{Br}}$, characterized the kinetics of the reductive elimination (rate constant k_{2Br}). $d[\mathbf{12}_{Br}]/dt = -d[\mathbf{11}_{Br}]/dt = k_{2Br}[\mathbf{11}_{Br}]$ with $dx'/x' = -k_{2Br}t$.

The kinetic law for the reductive elimination is $\ln x' = -k_{2Br}t$ ($x' = (i_{lim} - i)/i_{lim}$; i_{lim} = oxidation current of the Pd(II) complex $\mathbf{12_{Br}}$ at the end of the reductive elimination; i = oxidation current of $\mathbf{12_{Br}}$ at t). The plot of $\ln x'$ against time was indeed linear (Figure 5). The value of k_{2Br} was calculated from the slope of the straight line.

A series of experiments was performed with three different concentrations of PhCH$_2$Br and the rate constants k_{2Br} determined as described above. The three values of k_{2Br} did not depend on the PhCH$_2$Br concentration within the accuracy of their determination, attesting to a zero-order reaction for PhCH$_2$Br, as expected for a reductive elimination (Scheme 4). An average value for the rate constant of the reductive elimination was then determined.

$$k_{2Br} = 6(\pm 1)\times 10^{-4}\ \text{s}^{-1}\ \text{(DMF, 29 °C)} \qquad (3)$$

The slow reductive elimination did not interfere in the kinetics of the oxidative addition for the PhCH$_2$Br concentration range investigated here (0.03−0.12 M): $k_{1Br}[PhCH_2Br] \gg k_{2Br}$. Moreover, the Pd(II) complex $\mathbf{12_{Br}}$ did not undergo any oxidative addition to PhCH$_2$Br (although present in excess

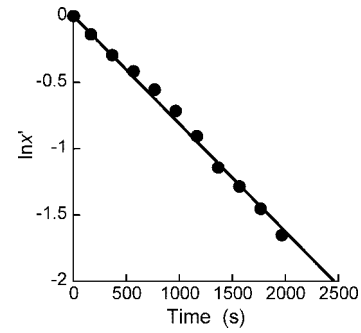

Figure 5. Kinetics of the formation of the Pd(II) complex $\mathbf{12_{Br}}$ generated by a reductive elimination from the Pd(IV) complex $\mathbf{11_{Br}}$ (formed by oxidative addition of PhCH$_2$Br (0.57 M) to the Pd(II) complex **10** (3 mM): decreasing part of Figure 4a), as monitored by amperometry at a rotating gold disk electrode polarized at +1 V, in DMF at 29 °C (increasing part of Figure 4a). Variation of $\ln x'$ against time ($x' = (i_{lim} - i)/i_{lim}$; i_{lim} = oxidation current of the Pd(II) complex $\mathbf{12_{Br}}$ at the end of the reductive elimination; i = oxidation current of $\mathbf{12_{Br}}$ at t).

(13) (a) Byers, P. K.; Canty, A. J.; Crespo, M.; Puddephatt, R. J.; Scott, J. D. *Organometallics* **1988**, *7*, 1363–1367. (b) Byers, P. K.; Canty, A. J.; Skelton, B. W.; Traill, P. R.; Watson, A. A.; White, A. H. *Organometallics* **1992**, *11*, 3085–3088. (c) Byers, P. K.; Canty, A. J.; Honeyman, T.; Skelton, B. W.; White, A. H. *J. Organomet. Chem.* **1992**, *433*, 223–229. (d) de Graaf, W.; Boersma, J.; Smeets, W. J. J.; Spek, A. L.; van Koten, G. *Organometallics* **1989**, *8*, 2907–2917. (e) van Asselt, R.; Rijnberg, E.; Elsevier, C. J. *Organometallics* **1994**, *13*, 706–720. (f) van Belzen, R.; Hoffmann, H.; Elsevier, C. J. *Angew. Chem., Int. Ed. Engl.* **1997**, *36*, 1743–1745.

(14) (a) Bard, A. J.; FaulknerL. R. In *Electrochemical Methods*, 2nd ed.; John Wiley & Sons: New York, 2001; pp 516−521. (b) Fauvarque, J. F.; Pflüger, F.; Troupel, M. *Organomet. Chem.* **1981**, *208*, 419–427.

during its formation) within the time scale of the reductive elimination. This means that the Pd(II) complex **10** was considerably more reactive with $PhCH_2Br$ than the Pd(II) complex $\mathbf{12_{Br}}$,[15b] thus pointing out the key importance of the metallacyclic aryl and norbornyl C−Pd bonds in Pd(II) complex **10** to induce the oxidative addition.

Analogously to the oxidative addition of $PhCH_2Br$ to **10**, that of $PhCH_2Cl$ gave the Pd(IV) complex $\mathbf{11_{Cl}}$, which should undergo a C−C reductive elimination to give back a Pd(II) complex. The Pd(IV) complex $\mathbf{11_{Cl}}$ formed in the oxidative addition was characterized by ^{1}H NMR at −5 °C (Scheme 3) because it underwent reductive elimination at room temperature. Once the Pd(IV) complex $\mathbf{11_{Cl}}$ was generated in the oxidative addition of $PhCH_2Cl$ to the Pd(II) complex **10** at 29 °C (as followed by amperometry at the rotating disk electrode polarized at +1 V), no oxidation current was detected at longer times. The cyclic voltammogram did not exhibit any oxidation wave in the range of potentials investigated here (less positive than +1.0 V), suggesting that the oxidation wave of the expected Pd(II) complex $\mathbf{12_{Cl}}$ should be located at more positive potential than +1.0 V and consequently could not have been detected during a kinetic experiment similar to that of Figure 4.

Conclusion

Summing up, it can be stated that the kinetic pathway of the palladium-catalyzed alkylation of aryl with benzyl halides is in agreement with the key steps of the mechanism of the catalytic reactions (**3** → **4** → **5** in Scheme 2), proposed on the basis of the isolation of a Pd(IV) complex with phenanthroline as ligand. It has been established that the Pd(II) metallacyclic complex **10** undergoes oxidative addition to benzyl bromide or chloride in DMF to generate Pd(IV) complexes with the reactivity order $PhCH_2Br$ > $PhCH_2Cl$. The oxidative addition of $PhCH_2Br$ is followed by a slow C−C reductive elimination from the benzyl-Pd(IV) complex, which gives back a Pd(II) complex. The rate constants of the oxidative additions and the reductive elimination have been determined in DMF. These results are of general interest because they add important information to the ongoing debate on the competition of the mechanism involving a Pd(IV) complex and the one based on transmetalation between Pd(II) complexes.[16] Whether the preference for the Pd(IV) complex reported here also holds for aromatic arylation, it requires further study, however, with a suitable model.

Experimental Section

Chemicals. DMF was distilled from calcium hydride and kept under argon. The benzyl chloride and bromide were commercial and used after filtration on alumina. Complex **10** was synthesized according to a published procedure.[6a]

Electrochemical Setup and Electrochemical Procedure for Cyclic Voltammetry. Experiments were carried out in a three-electrode cell connected to a Schlenk line. The cell was equipped with a double envelope to have a constant temperature (Lauda RC20 thermostat). The working electrode consisted of a gold disk (d = 0.5 mm). The counter electrode was a platinum wire of ca. 1 cm^2 apparent surface area. The reference was a saturated calomel electrode separated from the solution by a bridge filled with a solution of nBu$_4$NBF$_4$ (0.3 M) in 3 mL of DMF. Then 8 mL of DMF containing the same concentration of supporting electrolyte was poured into the cell. A 10.9 mg amount of complex **10** (0.024 mmol, 3 mM) was then added. Cyclic voltammetry was performed at a scan rate of 0.5 V s^{-1}.

General Procedure for the Kinetics of the Oxidative Addition As Monitored by Amperometry. Experiments were carried out in the same cell as above at 29 °C. A 15 mL amount of DMF containing 0.3 M nBu$_4$NBF$_4$ was poured into the cell. Then 20.5 mg (0.045 mmol, 3 mM) of complex **10** was introduced into the cell. A rotating gold disk electrode (d = 2 mm, EDI 65109 (Radiometer Analytical) with an angular velocity of 105 rad s^{-1} (Radiometer Analytical controvit)) was polarized at +1 V on the plateau of the oxidation wave of complex **10** at O_1 (Figure 1b). It was checked that the oxidation current was constant within at least 5 min. The appropriate amount of the benzyl bromide or chloride was then added into the cell, and the decrease of the oxidation current was recorded versus time up to 100% conversion.

General Procedure for the Kinetics of the Reductive Elimination As Monitored by Amperometry. The kinetics of the reductive elimination was followed under the same experimental conditions reported above for the oxidative addition using the same rotating gold disk electrode polarized at +1 V. Once the oxidative addition of $PhCH_2Br$ (1.022 mL, 8.55 mmol, 0.57 M) to 20.5 mg (0.045 mmol, 3 mM) of complex **10** was over, the increase of the oxidation current of the Pd(II) complex $\mathbf{12_{Br}}$ was recorded versus time up to 100% formation (increasing part of Figure 4a).

Characterization of Complex $\mathbf{11_{Cl}}$. By adding benzyl chloride (3.6 μL, 0.031 mmol) to complex **10** (9 mg, 0.019 mmol) in 0.6 mL of $CDCl_3$ at room temperature, a new compound, $\mathbf{11_{Cl}}$, was slowly formed. Its formation was followed by ^{1}H NMR spectroscopy, which showed its presence in solution in ca. 1:0.8 molar ratio with the starting complex **10** after 60 min. After this time complex $\mathbf{11_{Cl}}$ was characterized by NMR spectroscopy via COSY, NOESY, and TOCSY experiments at −5 °C using a Varian INOVA 600 spectrometer in no spinning mode (see the ^{1}H NMR spectrum in the Supporting Information). After longer times, $\mathbf{11_{Cl}}$ began to decompose, making the spectrum more complex. ^{1}H NMR (600 MHz, $CDCl_3$, 268 K): δ 8.68 (H2′, d, J = 4.4 Hz), 8.43 (H11, d, J = 7.7 Hz), 8.38 (H4′, d, J = 7.9 Hz), 8.32 (H7′, d, J = 8.1 Hz), 7.93−7.86 (H5′, H6′, H2″, H6″, m), 7.67 (H3′, dd, J = 7.9, 4.9 Hz), 7.44−7.31 (H8′, H3″, H4″, H5″, m), 7.22 (H10, t, J = 7.3 Hz), 7.18 (H9, t, J = 7.3 Hz), 7.07 (H8, d, J = 7.3 Hz), 6.54 (H9′, d, J = 4.8 Hz), 4.62 (benzylic-H, d, J = 7.8 Hz), 3.98 (H2, d, J = 7.0 Hz), 3.43 (H3, d, J = 7.0 Hz), 3.31 (benzylic-H, d, J = 7.9 Hz), 2.40−2.35 (H4, m), 1.51−1.40 (H5 *exo*, m), 1.32−1.20 (H5 *endo*, m), 1.13 (H7 *syn*, d, J = 9.3 Hz), 1.00−0.83 (H6 *exo*, H1, H6 *endo*, m), 0.49 (H7 *anti*, d, J = 9.3 Hz).

Characterization of Complex $\mathbf{12_{Br}}$. To 3 mL of a CH_2Cl_2 solution of **10** (50 mg, 0.11 mmol) at 0 °C was added benzyl bromide (21 mg, 0.12 mmol) dissolved in 1 mL of CH_2Cl_2 under nitrogen. The reaction mixture was allowed to reach room temperature under stirring and was maintained at room temperature for an additional 3 h. Removal of most of the solvent and

(15) (a) At the end of the reductive elimination, the oxidation current of the Pd(II) complex $\mathbf{12_{Br}}$ reached a value of i_{lim} = 2.2 μA, which was about half of the initial oxidation current of the Pd(II) complex **10** (Figure 4a). This might be due to a lower diffusion coefficient D for $\mathbf{12_{Br}}$ compared to that of **10** because the latter is more condensed (the current at a rotating electrode is proportional to $D^{2/3}$)[14a] associated with an oxidation for $\mathbf{12_{Br}}$ involving fewer electrons (e.g., n = 0.5, if a dimerization process occurs during the electron transfer) than the one-electron oxidation observed for **10**.[11] (b) The peak potentials E^p of **10** and $\mathbf{12_{Br}}$ look close to each other (Δ = 35 mV at a scan rate of 0.5 V s^{-1}) but cannot be compared to evaluate the relative ability of complexes **10** and $\mathbf{12_{Br}}$ to undergo oxidative addition (whenever it is indicative) because peak potentials E^p might be very different from their respective standard potentials E^0. The oxidation peaks of complexes **10** and $\mathbf{12_{Br}}$ were fully irreversible at the scan rate of 0.5 V s^{-1}. No attempt was made to increase the scan rate to determine their respective standard potentials E^0, which could be compared and might be very different from each other. See: Bard, A. J.; Faulkner L. R. In *Electrochemical Methods*, 2nd ed.; John Wiley & Sons: New York, 2001; pp 234−236.

(16) (a) Cárdenas, D. J.; Martín-Matute, B.; Echavarren, A. M. *J. Am. Chem. Soc.* **2006**, *128*, 5033–5040. (b) Mota, A. J.; Dedieu, A. *Organometallics* **2006**, *25*, 3130–3142.

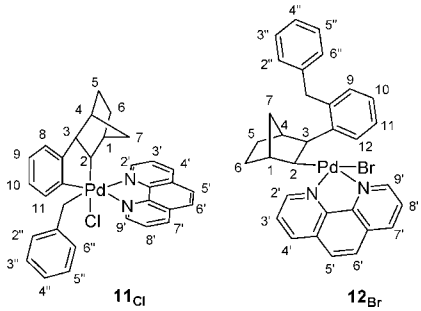

11$_{Cl}$ **12**$_{Br}$

slow addition of diethyl ether led to the formation of a yellow-orange powder. The mixture was cooled at ca. −15 °C to favor precipitation of complex **12**$_{Br}$ (51 mg, 0.08 mmol, 74%), which was filtered and dried under vacuum. ^{1}H NMR (300 MHz, $CDCl_3$, 293 K): δ 9.70 (dd, J = 4.8, 1.5 Hz, 1H, H2′), 9.66 (dd, J = 7.7, 1.0 Hz, 1H, H12), 9.05 (dd, J = 4.8, 1.3 Hz, 1H, H9′), 8.40 (dd, J = 8.1, 1.5 Hz, 1H, H4′), 8.32 (dd, J = 8.1, 1.5 Hz, 1H, H7′), 7.92, 7.89 (AB system, J = 8.0 Hz, 2H, H5′, H6′), 7.73 (dd, J = 8.1, 4.8 Hz, 1H, H8′), 7.38−7.16 (m, 4H, H3′, H2″, H4″, H6″), 7.16−7.08 (m, 2H, H3″, H5″), 7.05−6.95 (m, 1H, H11), 6.84−6.71 centered at 6.81 (m, 2H, H10, H9), 4.14, 4.05 (AB system, J = 16.1 Hz, benzylic-H, 2H), 3.32 (d further split, J = 7.6 Hz, 1H, H7 *syn*), 3.24 (br d, J = 7.1 Hz, 1H, H2), 3.09 (br d, J = 7.1 Hz, 1H, H3), 2.50−2.43 (m, 1H, H1), 1.87−1.81 (m, 1H, H4), 1.64−1.45 (m, 1H, H6 *exo*), 1.32−1.15 (m, 2H, H7 *anti*, H5 *exo*), 0.98−0.81 (m, 1H, H6 *endo*), 0.55−0.42 (m, 1H, H5 *endo*). Anal. Calcd for $C_{32}H_{29}BrN_2Pd$: C, 61.21; H, 4.66; N, 4.46. Found: C, 61.12; H, 4.50; N, 4.38.

Acknowledgment. This work has been supported in part by the Centre National de la Recherche Scientifique (UMR CNRS-ENS-UPMC 8640), the Ministère de la Recherche (Ecole Normale Supérieure), and the Ministero dell'Università e della Ricerca Scientifica e Tecnologica (Cofinanziamento MIUR, 2006031888).

Supporting Information Available: ^{1}H NMR spectrum of **11**$_{Cl}$. This material is available free of charge via the Internet at http://pubs.acs.org.

OM800015X